MIT Open Access Articles

Molecular influence in high-strain-rate microparticle impact response of poly(urethane urea) elastomers

Molecular Influence in High-Strain-Rate Microparticle Impact Response of Poly(urethane urea) Elastomers

David Veysset[1,2], Alex J. Hsieh[1,3*], Steven E. Kooi[1], and Keith A. Nelson[1,2].

[1]Institute for Soldier Nanotechnologies, MIT, Cambridge, Massachusetts 02139, USA

[2]Department of Chemistry, MIT, Cambridge, Massachusetts 02139, USA

[3]U.S. Army Research Laboratory, RDRL-WMM-G, Aberdeen Proving Ground, Maryland 21005-5069, USA

Abstract

The dynamic deformation response of select model poly(urethane urea) elastomers (PUU) at high strain rates is investigated via an all-optical laser-induced projectile impact test (LIPIT). LIPIT measurements allow the direct visualization of the impact of micro-projectiles (silica spheres) on substrates and *in-situ* characterization, including depth of penetration and the extent of rebound of the micro-projectiles. PUUs are proven to be robust and the silica spheres are observed to rebound from them upon impact. In addition, for PUUs a strong correlation was noted between the coefficient of restitution and the maximum depth of penetration. Also, the coefficient of restitution data is comparable to that of glassy polycarbonate (PC), which is in great contrast to the comparison of the corresponding ambient storage modulus data obtained via dynamic mechanical analysis at 1 Hz. We hypothesize that high-rate deformation-induced glass transition is a plausible molecular relaxation mechanism towards macroscopic, dynamic stiffening/strengthening in PUUs.

Keywords: laser-induced particle impact test (LIPIT); micro-ballistics; poly(urethane urea) elastomers; coefficient of restitution; depth of penetration; segmental dynamics; high-rate deformation-induced glass transition

*Corresponding author, Email: alex.j.hsieh.civ@mail.mil, Phone: 410-306-2292, Fax: 410-306-0676

1. Introduction

Better understanding of the deformation of materials in extreme dynamic environments remains a great challenge among the research community across the Department of Defense (DoD) and academia. Recently, the development of a novel laser-induced particle impact platform has shown the capability of providing real-time in-situ visualization of the deformation response in a broad range of materials, from polystyrene-polydimethylsiloxane diblock copolymers (PS-b-PDMS) to graphene [1–4]. Upon impact, it was shown that PS-b-PDMS, consisting of a 40 nm periodic glassy-rubbery layered nanostructure, exhibited penetration and embedment of micro-spheres of silica particles, along with distinct microstructural changes, where the dissipation of impact energy was attributed to plausible pathways including layer kinking, layer compression, extreme chain conformational flattening, domain fragmentation, and segmental mixing [1]. Meanwhile, work on LIPIT measurements of multilayer graphene revealed the presence of strong delocalization behavior and correspondingly, the potential of enhanced specific delocalized penetration energy, about eight to ten times higher than that of steel [2]. In addition, recent observations further highlighted the capability of LIPIT to enable differentiation with respect to the influence of molecular mechanism on the high strain-rate impact deformation response between select model poly(urethane urea), PUU, and polydimethylsiloxane (PDMS) elastomers [3].

PUUs are composed of urethane and urea linkages; the versatile chemistry and intrinsic intermolecular hydrogen bonding in these segmented PUUs like in segmented polyurethane and polyurea elastomers give rise to complex microstructure and a broad range of physical and mechanical properties [5–13]. The motivation towards hierarchical elastomers was derived from a novel molecular mechanism – high-rate deformation-induced glass transition, revealed by Bogoslovov et al. [14], which was successfully used to explain why a thin layer of polyurea coating on a steel plate was capable of providing ballistic protection against penetration by a 50 cal. bullet [15]. These elastomeric materials have regained significant interest particularly for their potential in the areas of enhanced ballistic impact protection and shock wave mitigation capability [8,12–19]. However, challenges remain to fully understand the efficacy of molecular attributes that would provide guidance to enable better selection of the proper high performance elastomers required for the overall dynamic impact deformation optimization. For example, Hsieh et al. successfully characterized ultrahigh molecular weight polyethylene (UHMWPE) prepreg and composite materials, and found a strong correlation between the molecular dynamics of matrix elastomers

used in the prepregs and the macroscale back-face-deformation (BFD) response of the corresponding composites observed upon ballistic impact. In practice, ballistic helmets are produced through consolidation of prepreg materials, where the UHMWPE prepregs of interest are composite materials consisting of UHMWPE fibers in the form of unidirectional, 0/90/0/90, wherein each fiber is impregnated with either polyurethane-based or Kraton®-based matrix elastomers. These prepreg materials are in the form of sheets, where the role of matrix elastomers is to bond the fibers. It was shown that UHMWPE prepreg composites composed of polyurethane matrix elastomers out-performed in the BFD reduction compared to those composed of Kraton® based matrix elastomers [20]. These results are of critical importance when the performance requirements for helmets are considered; it is noteworthy that the extent of BFD upon impact is detrimental if the deformation exceeds the helmet standoff (distance from helmet to head) as it can transfer large forces to the skull, thus potentially causing great concern towards blunt impact trauma [21,22].

With respect to the molecular attributes that are important towards energy absorption and dissipation, it is envisioned that for hierarchical elastomers multiple time constants for energy relaxation and dissipation are required, which could be associated with various relaxation modes within either microphase-separated or a co-continuous phase domains. Thus, a full multiscale characterization approach is required for building a better scale-bridging understanding of the segmental dynamics in order to provide a full picture of the dynamic response, particularly when these hierarchical elastomers are exposed to a broad range of external stimuli, ranging from ballistic impact, shock and other extreme dynamic environments, regardless of being in the bulk or as matrix elastomers in composites.

Segmental relaxation dynamics can be characterized in dielectric measurements, in the case where absorption maximum occur when dipole relaxation time, τ, (due to molecular relaxation) matches the inverse frequency $(1/\omega)$ of the alternating electric field impulse, i.e. when $\omega\tau = 1$ [23]. Broadband dielectric spectroscopy measurements revealed a drastic difference in dielectric relaxation and the corresponding segmental mobility among three select PUUs, which consist of 4,4'-dicyclohexylmethane diisocyanate (HMDI), diethyltoluenediamine (DETA), and poly(tetramethylene oxide) (PTMO), having the same stoichiometric ratio, 2:1:1 of [HMDI]:[DETA]:[PTMO] but varying in the molecular weight of PTMO (650, 1,000 and 2,000 g/mol), namely 211-650, 211-1000, and 211-2000, respectively [8]. The 211-650 PUU exhibited a strong relaxation at ~ 8 Hz along with a second loss maximum at ~ 4,600 Hz. The former

presumably corresponds to the most phase-mixed regions, where the formation of co-continuous, highly intermolecular hydrogen bonded hard segment (HS) / soft segment (SS) networks could be a plausible attribute. For 211-1000, a strong relaxation occurred at ~21,200 Hz, and additionally there was a small shoulder at ~ 8-10 Hz, though the latter was found to be less significant than the strong relaxation seen in 211-650 [8]. However, for 211-2000, it was not until ~ 10^6 Hz that an apparent relaxation was noted. The segmental mobility calculated based on broadband dielectric analysis varied over five orders of magnitude among these three PUUs, where the segmental relaxation time τ at 298 K was determined to be ~ 0.02 s, 7.5×10^{-6} s and 5×10^{-8} s for 211-650, 211-1000 and 211-2000, respectively [8]. Additionally, the trend in segmental dynamics associated with the glass transition of soft segments, determined from the dielectric measurements, appears to correspond very well with the phase-mixed relaxation data obtained from dynamic mechanical analysis (DMA) [8].

Furthermore, studies from solid-state nuclear magnetic resonance (ssNMR) spectroscopy measurements revealed new insight into the dynamics on the molecular level among the three select PUUs, 211-650, 211-1000, and 211-2000 [24,25]. In ssNMR, the time-domain wideline separation (TD-WISE) data clearly elucidated that segmental dynamics associated with soft segments in the phase-mixed regions were at least an order of magnitude slower than those obtained for the mobile, soft-segment-rich regions in these PUU elastomers [8,25]. Thus, when considering dynamic strengthening in a temporal scale on the order of microsecond at ambient temperature, it would most likely be dominated by the molecular motion associated with soft segments within the phase-mixed regions [8,24,25].

Impulsive stimulated scattering (ISS) measurements, on the other hand, allow for characterization of relaxation behavior at the nanoscale, where absorption of two laser excitation pulses, which are crossed in the sample, results in localized sample heating and fast thermal expansion, which subsequently generates a coherent acoustic wave with oscillation on the order of 300 MHz frequency (~ 10^8/s) [26]. In ISS, the speed of sound can be obtained based on the acoustic wave oscillation measurements, where the frequency of impulse is roughly on the same order of the segmental mobility ($1/\tau$) of PUU 211-2000 but much greater than that of PUU 211-1000 and 211-650. Thus, it is expected that high-rate deformation-induced glass transition would occur in these PUUs. This was validated from the apparent (frequency-dependent) modulus measurements, which was calculated based on the respective speed of sound derived from the 300 MHz acoustic wave oscillation measurements in ISS. For example, the apparent modulus of

PUU 211-650 from ISS was only about 60% larger than that of PUU 211-2000, whereas for the former the ambient storage modulus measured at 1 Hz in DMA was about 17 times larger than that of the latter. Additionally, in ISS all of these PUUs exhibit about the same decay time ~ 8 ns, regardless of their compositions. It is noteworthy that even for the most rubbery PUU 211-2000 the calculated speed of sound, 1770 m/s, was still faster than that of PDMS, 1074 m/s, presumably due to the fact that PUU 211-2000 exhibits a greater dynamic stiffening response than PDMS. This is consistent to the aforementioned molecular influence upon high strain-rate impact response observed under LIPIT [3].

To further validate our hypothesis with respect to the influence of molecular mechanism upon dynamic deformation response of hierarchical elastomers at large strains and at the nano-second timescale, a better choice of *in-situ* experimental techniques is needed. In this work, we exploit LIPIT for a comprehensive investigation of the supersonic microparticle impact response of PUU elastomers, where real-time characterization of mode of deformation, including the extent of depth of penetration and extent of projectile rebound, will be used to determine the coefficient of restitution with respect to the PUU molecular composition and projectile impact velocity.

2. Experimental
2.1. Materials

Select model PUU elastomers composed of 4,4'-dicyclohexylmethane diisocyanate (HMDI), diethyltoluenediamine (DETA), and poly(tetramethylene oxide) (PTMO), with three different molecular weight (MW) of the PTMO soft segment (SS), 650, 1,000 and 2,000 g/mol, prepared via a two-step, pre-polymer synthesis [5], were chosen for this study. In the sample nomenclature, the numerals 'xyz' refer to the molar ratio of HMDI:DETA:PTMO, and the succeeding '650', '1000', and '2000' refer to the MW of PTMO as 650, 1,000, and 2,000 g/mol, respectively. In this work, 211-650, 532-1000, 431-2000, 211-1000, 321-2000, and 211-2000 were chosen for study, and Table 1 lists the composition along with the weight percentage (wt.%) values for both HS_u and HS_{uu} for the select PUUs. The hard segment content HS_u corresponds to the calculation based on the Flory's formula and only accounts for the portion of diisocyanate that reacts with diamine, whereas the HS_{uu} calculation also accounts for the additional portion of diisocyanate that reacts with the polyether diol [27]. These hard segment wt.% values will be differentiated when used to interpret the molecular influence on the dynamic material response. The

5

impact response of PUUs is also compared with a ductile glassy polycarbonate (Lexan® PC).

Table 1. Composition and the calculated values of hard segment content of select model PUUs.

Materials	Molar Ratio of [HMDI]: [DETA]: [PTMO]	MW(g/mol) of PTMO	Wt.% of hard segment	
			HS_u	HS_{uu}
211-650	2:1:1	650	33	52
532-1000	5:3:2	1,000	34	48
431-2000	4:3:1	2,000	37	44
211-1000	2:1:1	1,000	26	41
321-2000	3:2:1	2,000	28	36
211-2000	2:1:1	2,000	16	26

2.2. Laser-induced Projectile Impact Test (LIPIT)

The high-strain-rate deformation response of selected elastomers and glassy polymeric materials was investigated by using the laser-induced projectile impact test (LIPIT) developed by Lee et al. [1] and recently upgraded with real-time observation capabilities by Veysset et al. [3]. With respect to high-strain-rate deformation, most of the conventional characterization techniques, such as the split-Hopkinson pressure bar impact [28] or macro-ballistic test, require large scale samples, whereas LIPIT enables the investigation of micro-scale deformations at nanosecond timescales for much smaller samples [1,2]. Here, we observed the dynamic response *in-situ* of 211-650, 532-1000, 431-2000, 211-1000, 321-2000, and 211-2000 samples under high strain-rate micro-sphere impact at speeds varying from approximately 200 m/s to 800 m/s.

The launching pad assembly consists of a 210 micron thick glass substrate, a 60 nm gold film for laser absorption, a 5 micron cross-linked PDMS layer, and a sub-monolayer of silica micro-spheres (D = 7.38 μm ± 0.24 μm) deposited on top of the assembly as described in Refs [2,3]. Upon laser ablation of the gold film using a 300-picosecond duration, 800-nm wavelength laser pulse focused in a region of about 50-micron diameter, the PDMS layer expands and propels the particles into free space. The particle speed can be adjusted from 200 m/s to 800 m/s by varying the laser pulse energy from 0.15 to 0.30 mJ (Fig. 1). Using a high-speed camera (SIMX16, Specialized Imaging), that consists of 16 CCDs independently triggerable with exposure times as short as 5 ns and variable inter-frame times, we visualized the micro-spheres as they impacted the surface of the samples and subsequently rebounded, providing insight into

the high strain rate deformation response of these selected polymeric materials. Both impact and rebound trajectories as well as their corresponding velocities and penetration depth were extracted directly from the 16-image videos. A more detailed description of the imaging setup and image analysis can be found in Ref. [3].
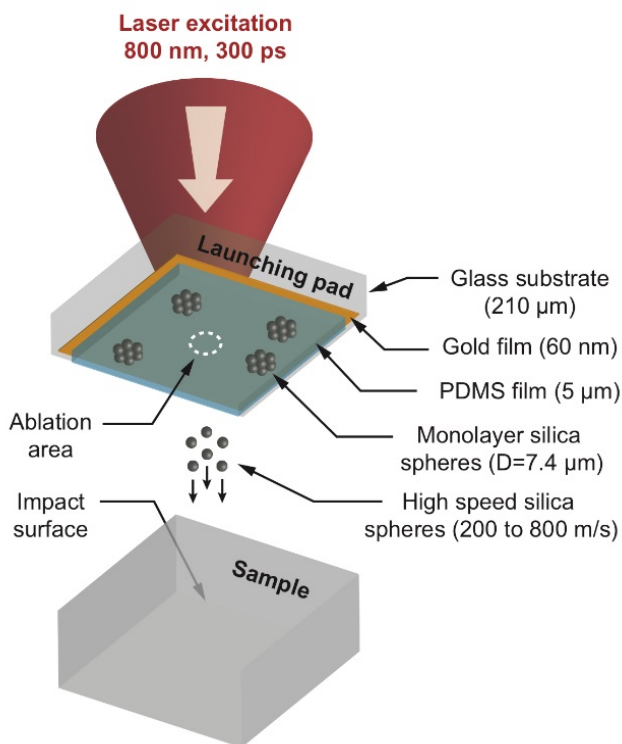

Fig. 1. Schematic illustration of the laser-induced particle impact test. A single 300 picosecond duration, 800 nm wavelength laser pulse with variable energy (up to 0.30 mJ) is focused onto a laser absorbing polymer layer with a laser exposed area of 50 μm in diameter. Silica particles (D = 7.38 μm ± 0.24 μm) deposited as a sub-monolayer on top of the PDMS layer are accelerated upon rapid expansion of the gas produced by laser ablation of the gold film. The projectiles are ejected into free space with controllable speeds, depending on laser energy, after which they impact a target sample at near-normal incidence (± 5°). The distance between the glass assembly or launching pad and the target is approximately 1.0 mm.

2.3. Dynamic Mechanical Analysis (DMA)

The DMA measurements were performed on a TA Instruments Q800 Dynamic Mechanical Analyzer. Both PUU and PC specimens were tested in an oscillatory tensile mode at a heating rate of 2 °C/min and a frequency of 1 Hz.

7

3. Results

3.1. High strain-rate impact

Fig. 2 displays a representative sequence of images showing the dynamic impact of micro-spheres upon 211-650 and 321-2000 PUU samples, where a distinct difference in material response was noted. On one hand, the 211-650 sample, the most rigid PUU at ambient temperature, exhibited a shallow particle penetration (about 4 µm) upon impact at 790 m/s and a fast projectile rebound of 195 m/s. On the other hand, the 321-2000 sample, a more flexible PUU at ambient temperature, showed a deeper penetration of particle to about 9 µm upon impact at 730 m/s and a slower particle rebound of 80 m/s. The strain-rates associated with these impacts were estimated as v/h [29], where v is the impact velocity and h the depth of penetration, to be on the order of 2.0×10^8/s and 8.1×10^7/s for 211-650 and 321-2000, respectively. It was also noted that microparticles with speeds ranging from 600 m/s to 800 m/s impacting 211-2000 samples penetrated deeper than in 321-2000 samples and thereafter were expelled to the surface of the target where they eventually remained (see Ref. [3] and Fig 3a).

For PUU 211-2000, the most rubber-like among the select PUU elastomers, rebound of micro-spheres also occurs when impacted at relatively low speeds below 430 m/s. This clearly validates our hypothesis that PUU 211-2000 with ambient segmental relaxation time on the order of 10^{-8} s could presumably undergo high-rate deformation-induced glass transition upon impact via LIPIT at strain rates $\sim 10^8$/s. For illustration, we include the representative broadband dielectric relaxation data for PUU 211-2000 and 211-1000 as shown in Fig. 4a, reproduced from Ref. [3], to further elucidate the role of dynamic T_g, in comparison to the corresponding DMA data (Fig. 4b, reproduced from Ref. [5]), particularly with respect to the dynamic strengthening characteristics observed among these PUUs. It is noteworthy that the trend in the composition dependence of segmental relaxation based on the dielectric relaxation measurements corroborates very well with the corresponding phase-mixed soft segment T_g data observed in DMA. Additionally, for PUU 211-2000 the dynamic T_g corresponding to the segmental mobility $\sim 10^8$/s is indeed very close to ambient temperature determined based on the broadband dielectric spectroscopy relaxation data.
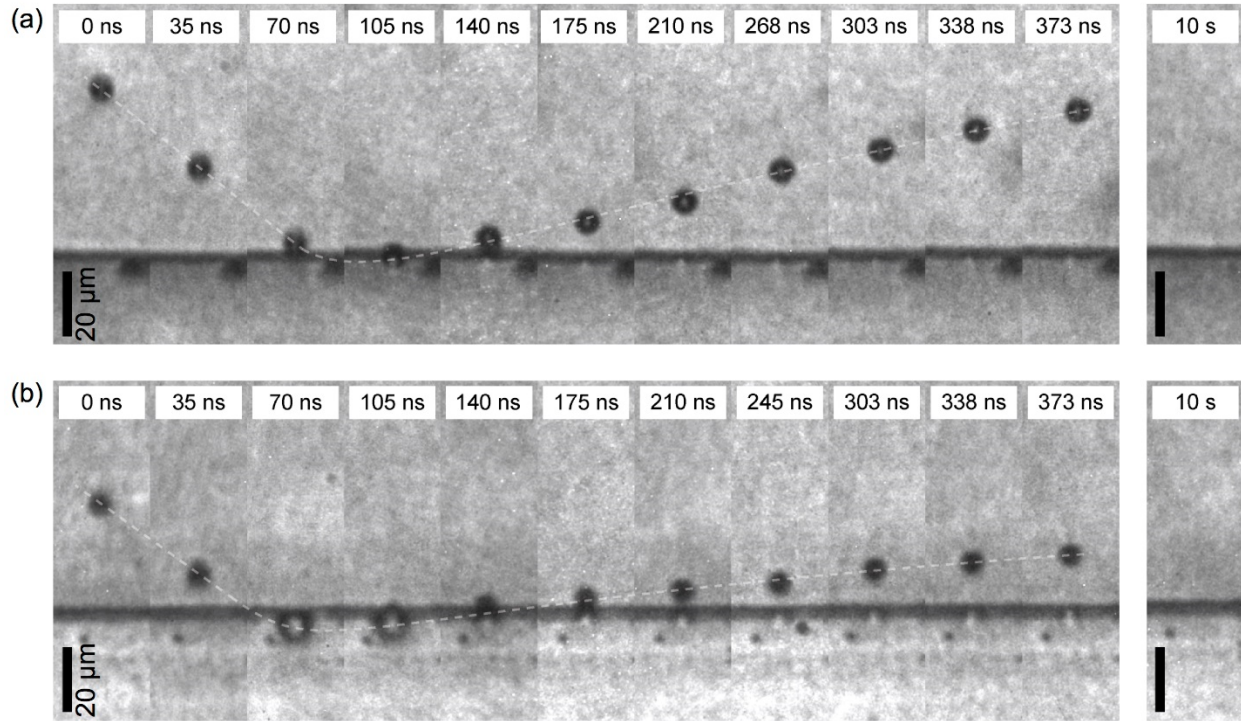
Fig. 2. Typical sequence of images recorded using a high-speed camera with 3-ns exposure time showing particle impact on (a) a 211-650 sample and (b) a 321-2000 sample. 11 out of 16 images recorded in real-time by the high-speed camera are presented here cropped from their initial size for the ease of comparison. The time stamps, shown at the top of the frames, indicate the delay in acquisition time relative to the first frame of the sequence. (a) A particle impacts a 211-650 sample with a speed of 790 m/s and almost instantaneously rebounds from the material surface with a speed of 195 m/s and with minimum penetration. (b) Unlike in 211-650, the particle impacting the 321-2000 sample at a speed of 730 m/s penetrates deeper in the sample and rebounds with a slower speed of 80 m/s. The images recorded about 10 seconds after impact show the sample surfaces with no apparent in-depth sample damage in both cases. The white dashed lines mark the approximate trajectories of the projectiles.

For comparison, LIPIT was also performed on a ductile glassy thermoplastic, polycarbonate (PC). Rebound of the micro-spheres from the PC sample surface occurs at relatively high velocities, similar to what was observed for 211-650. However, a drastic difference in the post-mortem surface morphologies was observed. No signs of post-mortem damage were observed after impacts on PUUs, including 211-650, 532-1000, 431-1000, 211-1000, 321-2000, and 211-2000; for the latter, the projectile sits on the sample's surface (Fig. 3a), whereas plastic deformation is predominant in PC (Fig. 3b). It is envisioned that material deformation upon microparticle impact could be very complex, where the influence of local

9

heating induced upon supersonic impact could be an important attribute and subsequently, the resultant thermal softening could also be a plausible pathway towards mitigating the formation of micro-cracks and permanent damage in PUUs and PC. Meanwhile, post-mortem observations of sample surfaces via SEM and confocal microscope did not reveal any sign of melting, which could otherwise be characterized by drawn fibril-like features. Having local temperature probes in-situ is beyond current experimental capabilities. However, it is our interest and goal to better discern with respect to the extent of impact induced heating locally or globally. Work towards numerical simulation of LIPIT impact events is currently pursued through collaboration with another group and this will be discussed in following publications. Even so, these observations suggest that upon impact even the most rubber-like 211-2000 appears to be much more robust and exhibits greater dynamic stiffening than the glassy PC.
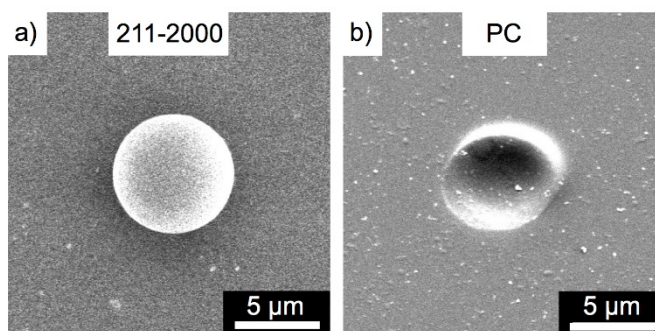

Fig. 3. Scanning electron microscope images reveal a great contrast in the mode of deformation between impacted materials under impact velocity range of 600-800 m/s. (a) For 211-2000, particles remain at the sample surface, and no permanent damage was evidenced after impact. (b) Permanent indent is observed on the surface of PC, indicative of plastic deformation.
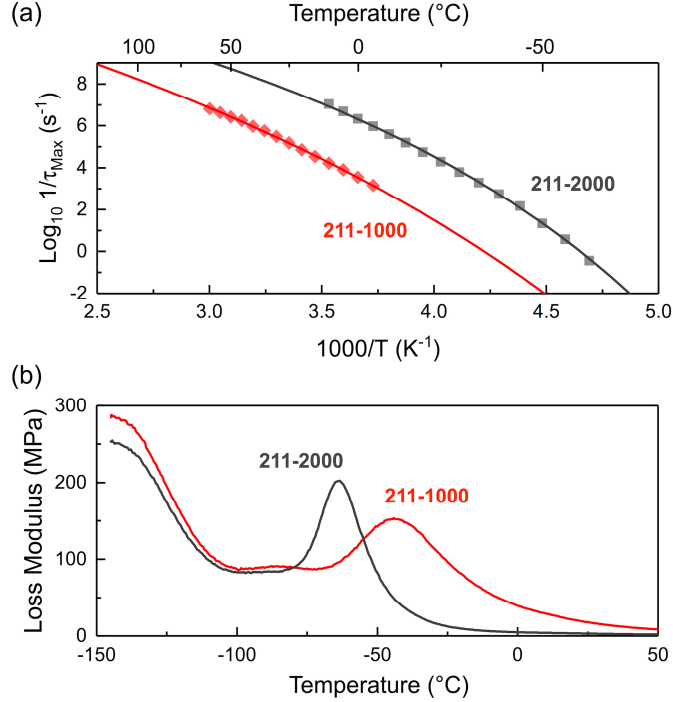
Fig. 4. (a) Arrhenius plot of segmental mobility ($1/\tau$) data obtained from broadband dielectric spectroscopy for PUU 211-1000 (red) and PUU 211-2000 (grey), reproduced from Ref. [3], and (b) Loss modulus vs. temperature data obtained for PUU 211-1000 (red) and PUU 211-2000 (grey) at 1 Hz in DMA, adapted from Ref. [5].

3.2. Composition effect

The dynamic T_g data from broadband dielectric relaxation measurements clearly reveal that PUU 211-2000 when impacted at strain rates $\sim 10^8$/s would presumably become glass-like and close to the same physical state as PUU 211-1000, 532-1000 and 211-650, in contrast to the great disparity when comparing the corresponding ambient storage modulus measured at 1 Hz in DMA [5,6] or ambient flow stress under quasi-static tension/compression measurements [8]. Thus, we carry out a comprehensive investigation via LIPIT to enable better discern and differentiation with respect to the influence of composition. Herein, we considered the coefficient of restitution. The coefficient of restitution, e, defined as the ratio between the rebound velocity v_r and the impact velocity v_i, or the reciprocal of the square root of the ratio of the corresponding kinetic energies, is widely used as an empirical parameter that measures the energy dissipation for collisional events involving rebound [30–36]. During projectile penetration, deceleration occurs and the kinetic energy of the incident projectile is converted to reversible elastic material

11

deformation and/or irreversible energy dissipation through stress waves generation, viscoelastic effects, and/or plastic deformation. The coefficient of restitution has been found to be particularly useful in studying glass transition in polymers and their pronounced viscoelastic nature in the transition [33,35–37]. In the case of a perfectly elastic collision, e is equal to one; however, it will decrease as the extent of energy dissipation increases. In the absence of rebound, as in the case of 211-2000 over the select range of impact velocity 500-800 m/s, the coefficient of restitution is equal to zero. It is noteworthy that the work of adhesion is inherently taken into account when calculating the coefficient of restitution. Adhesion contributes in reducing the particle rebound velocity as the particle exits from beneath the sample surface after impact. In the case of particle adhesion shown in Fig. 3a for PUU 211-2000, the adhesion presumably overcomes the elastic restoring forces that push the particle upward. As a result, the particle as shown remains at the surface of the sample.

For each impact event, particle trajectories before and after impact were extracted from the images sequences. Impact and rebound velocities were then directly derived from the trajectories. Fig. 5a depicts the extracted trajectories for the impact on 211-650 that is shown in Fig. 2a. The coefficient of restitution in this case is 0.25 for an impact velocity of 790 m/s. Fig. 5b shows the calculated coefficient of restitution for 211-650 as a function of particle impact speed. For relatively low speed impacts (about 200 m/s), the coefficient of restitution is less than unity attesting for inelastic collision. As the impact speed increases, the coefficient of restitution decreases further revealing the rate-dependent response of the PUU and therefore its viscoelastic and/or viscoplastic behavior. For the ease of visualization, the data was fitted with a three-parameter power law of the form:
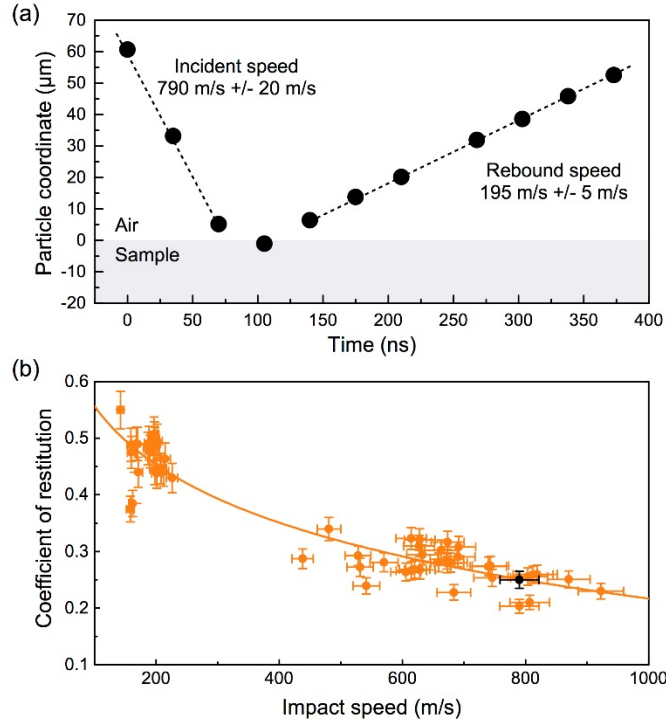
$$e = c_1 + c_2 v_i{}^{c_3} \qquad\qquad (1)$$

Fig. 5. (a) Particle trajectories pre- and post-impact extracted for the impact shown in Fig. 2a on 211-650. Impact and rebound speeds are determined through linear regression of the trajectories. The calculated coefficient of restitution of 0.25 is reported as a black dot in (b). (b) Coefficient of restitution vs. impact speed for 211-650. The data was fitted using Equation (1). The result of the fit is shown as a solid orange line.

We compare the coefficient of restitution as a function of impact speed for the select model PUUs, along with PC (Fig. 6). On one hand, PC, having the highest coefficient of restitution, dissipates, partly through plastic deformation (see Fig. 3b), the least amount of impact energy among all the tested samples. On the other hand, for the PUUs, the coefficient of restitution reflects a strong composition dependence and is determined as the following trend: 211-650 > 532-1000 > 431-2000 > 211-1000 > 321-2000 > 211-2000. For 211-650, rebound upon impact is consistent over the entire impact velocity test range. However, rebound of micro-spheres from 211-2000 occurs when impacted at relatively low speeds, but not at impact speeds higher than 430 m/s, where particles instead remained on the impacted surface (see Fig. 3a). Furthermore, it is noteworthy that these coefficient of restitution data strongly reflect the dynamic stiffening characteristics observed in PUUs, in comparison to PC, as the ambient storage modulus determined via DMA at 1 Hz is about ~0.35 GPa for 211-650, ~0.11 GPa for 211-1000 and 0.02 GPa for 211-2000, which are significantly lower than that of ~2 GPa for PC [8]. We attribute this dynamic

stiffening response of PUUs to the presence of a high-rate deformation-induced glass transition mechanism, which could presumably render even the most rubber-like PUU, 211-2000, to be prone to transition from rubbery towards leathery or close to glassy at strain rates on the order of 10^8 s^{-1}, as the segmental mobility of 211-2000 is reported to be about 10^7 s^{-1} at room temperature [3,8]. It is envisioned that the presence of multiple segmental relaxation modes associated with soft segments is key to the robust deformation response in these hierarchical PUU elastomers. This was revealed, as stated above, via ssNMR TD-WISE measurements, where dynamics at the molecular level of the phase-mixed rigid-SS was found at least an order of magnitude slower than that of the corresponding mobile-SS (those located in the SS-rich regions), regardless of the molecular weight of SS among the select model PUUs. As a result, we hypothesize that upon impact via LIPIT the rigid-SS of slower dynamics could enable dynamic stiffening while the mobile-SS would still accommodate dynamic relaxation. Meanwhile, supersonic-impact-induced heating could also promote self-healing presumably facilitated by the presence of intermolecular hydrogen bonding in PUUs.
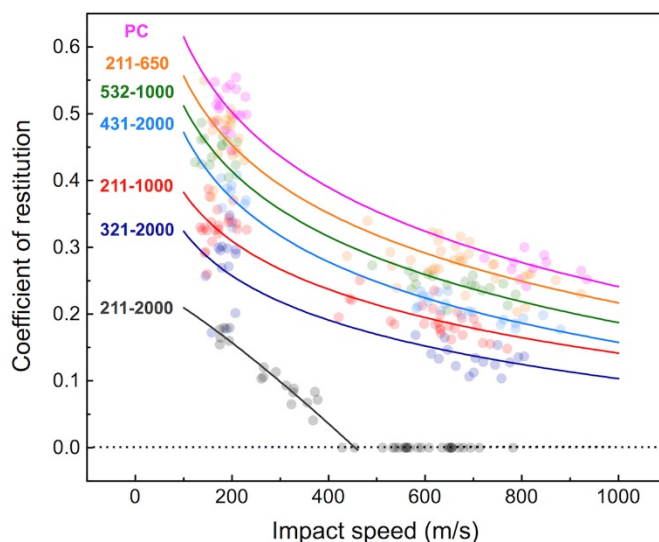

Fig. 6. Coefficient of restitution as a function of impact speed for select model PUU elastomers and PC.

The maximum penetration depth in PUUs was measured and averaged over the range of the highest impact speeds studied (600 to 800 m/s), which is shown in Fig. 7 as a function of HS_{uu}. Likewise, the coefficient of restitution data averaged over the same speed range are presented in Fig. 7. Both the trends in penetration depth and coefficient of restitution highlight a better corroboration with the effective hard segment content HS_{uu} than HS_u (see Supplementary Information) among these select model PUUs

14

impacted at high strain rates. This is consistent as the bidentate urea-urethane hydrogen bonding that contributes to greater phase mixing would presumably also undergo high-rate deformation-induced glass transition. As a result, HMDI moieties that are associated with the isolated hard segments dispersed among the soft domain matrix, yet not considered in the calculation of HS_u, would need to be taken into account with respect to their effective population. HS_{uu} aforementioned includes HMDI that reacts with PTMO to form the urethane linkages in addition to those reacted with the chain extender DETA to form the urea linkages [8]. Additionally, we note that the longitudinal speed of sound and apparent modulus of these PUUs, calculated based on ISS measurements at 300 MHz, showed the same trend with respect to HS_{uu} [38].
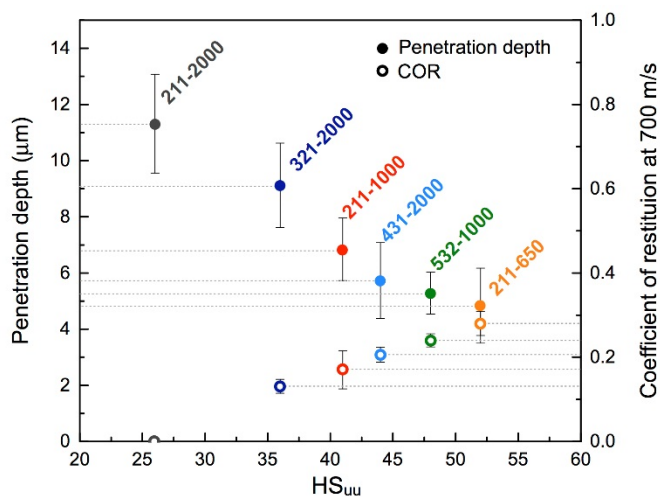

Fig. 7. Maximum penetration depth (solid-circles) and coefficient of restitution (open-circles) averaged for impact speeds between 600 m/s to 800 m/s as a function of HS_{uu}.

4. Discussion

To better discern and differentiate the molecular influence on the dynamic response over the temporal scale on the order of nanoseconds under LIPIT, we attempt to take into account the respective characteristics among the plausible molecular relaxation mechanisms between PUUs and PC.

For PUUs, we noted the influence of microstructure-mediated segmental dynamics strongly affecting the corresponding dynamic strain-rate hardening characteristics over a broad range of temporal scale $ms - \mu s$ [8], where the molecular motion associated with the soft segments was aforementioned characterized via DMA [5,6,8], broadband dielectric spectroscopy analysis [8] as well as ssNMR

[8,24,25]. In DMA, these PUUs exhibit multiple relaxation peaks which are associated with the soft segment glass transition temperatures, $T_{g,s}$, over the temperature range from -60°C to 50°C, dependent on the extent of phase mixing between soft and hard segments (representative loss modulus vs. temperature data for PUU 211-1000 and PUU 211-2000 are shown in Fig. 4b). Furthermore, broadband dielectric relaxation data clearly revealed the shift of $T_{g,s}$ as a function of frequency and, correspondingly, the aforementioned composition-dependent segmental dynamics (representative data for PUU 211-1000 and PUU 211-2000 are shown in Fig. 4a). We hypothesize that the presence of this segmental relaxation along with its strong frequency dependence are the key attributes where high-rate deformation-induced glass transition mechanism can be realized in PUUs. This could presumably be facilitated by the presence of an intermolecular hydrogen bonding, where a cooperative molecular relaxation throughout the physically-crosslinked network could be a plausible pathway. In contrast, PC despite its toughness does not exhibit a similar relaxation over the same temperature range in DMA as shown in Fig.8.
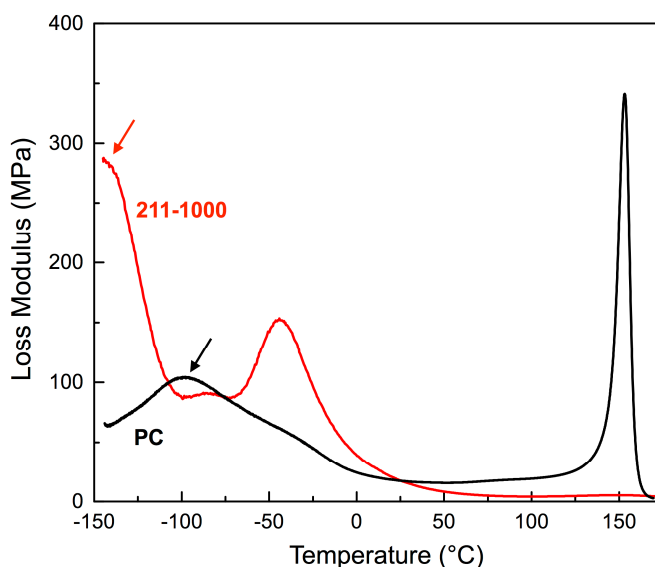

Fig. 8. Comparison of loss modulus vs temperature data obtained for PC (black) at 1 Hz in DMA with data for PUU 211–1000 (red) shown in Fig. 4b; arrows pointing to the respective γ-relaxations in PC and 211-1000.

For PC, a strong secondary γ-relaxation occurs at around -100°C at 1 Hz, which was reported to be the result of a cooperative molecular motion associated with several repeating units along the chain, where one of the dominant modes of relaxation was reported presumably the result of π-flips about the

aromatic-ring C_2 symmetry axis [39]. These flips were observed by dipolar rotational spin-echo ^{13}C ssNMR measurements that occurred over a broad range of frequencies centered about 300 kHz at room temperature [39]. For PUUs, there is also a γ-relaxation at about -150°C, regardless of compositions, which is presumably due to the crankshaft-like motion associated with the butylene spacer groups of PTMO. For the latter, recent ssNMR measurements showed that the ^{13}C T1 relaxation data obtained for the internal methylene moieties (27 ppm) of PTMO revealed the presence of predominantly fast-dynamics components about 0.2–0.3 s at ambient temperature under a Larmor frequency of 75 MHz, strongly indicative of local motion involving only the rotation of a few backbone bonds [25].

It is envisioned that for PUUs dynamic strain-rate hardening is predominantly facilitated by the presence of slow-dynamics components associated with the phase-mixed soft segments. Hence, even the most rubber-like 211-2000 would presumably undergo high-rate deformation-induced glass transition upon impact under LIPIT. These slow-dynamics components, on the other hand, are not readily available in PC, where energy absorption partly in the form of plastic deformation (as shown in Fig. 2b) is most likely accommodated by a cooperative, local molecular motion. These observations strongly suggest that PUUs, exhibiting rebound upon microparticle impact, are capable of greater dissipation of impact energy, in contrast to plastic deformation observed in the glassy PC, where supersonic-impact-induced softening could also be a factor for both PUUs and PC under the LIPIT. Meanwhile, the high-rate deformation-induced glass transition mechanism could be an important molecular pathway that can enable the design of robust hierarchical elastomers particularly towards dynamic strengthening and strain-rate hardening characteristics, which are of relevance to the materials performance optimization required for the extreme dynamic environments.

5. Conclusions

The molecular influence on dynamic deformation response of select model responsive hierarchical poly(urethane urea) elastomers and a glassy PC was investigated via a novel laser-induced particle impact test (LIPIT). This includes the evaluation of depth of penetration, projectile rebound and mode of deformation with respect to the influence of composition and impact speed. PUUs regardless of composition did not exhibit apparent plastic deformation like in PC, over a broad range of impact velocities under LIPIT. Results also indicated a strong correlation between the coefficient of restitution

and the maximum depth of penetration, both were strongly correlated with the hard segment content HS$_{uu}$ at high strain rates, where the coefficient of restitution was determined to be on the following trend: 211-650 > 532-1000 > 431-2000 > 211-1000 > 321-2000 > 211-2000. These coefficients of restitution data are comparable to that of glassy PC, which is in great contrast to the corresponding ambient storage modulus data obtained via DMA at 1 Hz. These observations clearly demonstrate the significance of segmental dynamics, where PUUs appear to be robust with a dynamic stiffening response causing the projectile to rebound, presumably facilitated by undergoing high-rate deformation-induced glass transition. In addition, the LIPIT is a viable multiscale characterization technique that can provide not only *in-situ* visualization of high strain-rate impact response, but also scale-bridging capability for better discern and validation with respect to the molecular dynamics on the temporal scale of ns for responsive hierarchical elastomers.

Acknowledgments

References

[1]   Lee J-H, Veysset D, Singer JP, Retsch M, Saini G, Pezeril T, et al. High strain rate deformation of layered nanocomposites. Nat Commun 2012;3:1164. doi:10.1038/ncomms2166.

[2]   Lee J-H, Loya PE, Lou J, Thomas EL. Dynamic mechanical behavior of multilayer graphene via supersonic projectile penetration. Science 2014;346:1092–6. doi:10.1126/science.1258544.

[3]   Veysset D, Hsieh AJ, Kooi S, Maznev AA, Masser KA, Nelson KA. Dynamics of supersonic microparticle impact on elastomers revealed by real–time multi–frame imaging. Sci Rep 2016;6:25577. doi:10.1038/srep25577.

[4]   Thevamaran R, Lawal O, Yazdi S, Jeon S-J, Lee J-H, Thomas EL. Dynamic creation and evolution of gradient nanostructure in single-crystal metallic microcubes. Science 2016;354:312–6.

doi:10.1126/science.aag1768.

[5] Sarva SS, Hsieh AJ. The effect of microstructure on the rate-dependent stress-strain behavior of poly(urethane urea) elastomers. Polymer 2009;50:3007–15. doi:10.1016/j.polymer.2009.04.025.

[6] Rinaldi RG, Hsieh AJ, Boyce MC. Tunable microstructures and mechanical deformation in transparent poly(urethane urea)s. J Polym Sci Part B Polym Phys 2011;49:123–35. doi:10.1002/polb.22128.

[7] Strawhecker KE, Hsieh AJ, Chantawansri TL, Kalcioglu ZI, Van Vliet KJ. Influence of microstructure on micro-/nano-mechanical measurements of select model transparent poly(urethane urea) elastomers. Polymer 2013;54:901–8. doi:10.1016/j.polymer.2012.12.018.

[8] Hsieh AJ, Chantawansri TL, Hu W, Strawhecker KE, Casem DT, Eliason JK, et al. New insight into microstructure-mediated segmental dynamics in select model poly(urethane urea) elastomers. Polymer 2014;55:1883–92. doi:10.1016/j.polymer.2014.02.037.

[9] Wang CB, Cooper SL. Morphology and properties of segmented polyether polyurethaneureas. Macromolecules 1983;16:775–86. doi:10.1021/ma00239a014.

[10] Abouzahr S, Wilkes GL, Ophir Z. Structure-property behaviour of segmented polyether-MDI-butanediol based urethanes: effect of composition ratio. Polymer 1982;23:1077–86. doi:10.1016/0032-3861(82)90411-6.

[11] Sheth JP, Aneja A, Wilkes GL, Yilgor E, Atilla GE, Yilgor I, et al. Influence of system variables on the morphological and dynamic mechanical behavior of polydimethylsiloxane based segmented polyurethane and polyurea copolymers: a comparative perspective. Polymer 2004;45:6919–32. doi:10.1016/j.polymer.2004.06.057.

[12] Yi J, Boyce MC, Lee GF, Balizer E. Large deformation rate-dependent stress-strain behavior of polyurea and polyurethanes. Polymer 2006;47:319–29. doi:10.1016/j.polymer.2005.10.107.

[13] Roland CM, Casalini R. Effect of hydrostatic pressure on the viscoelastic response of polyurea. Polymer 2007;48:5747–52. doi:10.1016/j.polymer.2007.07.017.

[14] Bogoslovov RB, Roland CM, Gamache RM. Impact-induced glass transition in elastomeric coatings. Appl Phys Lett 2007;90:221910. doi:10.1063/1.2745212.

[15] Roland CM, Fragiadakis D, Gamache RM. Elastomer–steel laminate armor. Compos Struct 2010;92:1059–64. doi:10.1016/j.compstruct.2009.09.057.

[16] Tekalur SA, Shukla A, Shivakumar K. Blast resistance of polyurea based layered composite materials. Compos Struct 2008;84:271–81. doi:10.1016/j.compstruct.2007.08.008.

[17] Fragiadakis D, Gamache R, Bogoslovov RB, Roland CM. Segmental dynamics of polyurea: Effect of stoichiometry. Polymer 2010;51:178–84. doi:10.1016/j.polymer.2009.11.028.

[18] Grujicic M, Pandurangan B, He T, Cheeseman BA, Yen CF, Randow CL. Computational investigation of impact energy absorption capability of polyurea coatings via deformation-induced glass transition. Mater Sci Eng A 2010;527:7741–51. doi:10.1016/j.msea.2010.08.042.

[19] Roland CM. Relaxation phenomena in vitrifying polymers and molecular liquids. Macromolecules 2010;43:7875–90. doi:10.1021/ma101649u.

[20] Hsieh AJ, Chantawansri TL, Hu W, Cain J, Yu JH. New insight into the influence of molecular dynamics of matrix elastomers on ballistic impact deformation in UHMWPE composites. Polymer 2016;95:52–61. doi:10.1016/j.polymer.2016.04.048.

[21] Vargas-Gonzalez LR, Walsh SM, Gurganus JC. Examining the Relationship Between Ballistic and Structural Properties of Lightweight Thermoplastic Unidirectional Composite Laminates (Technical Report No. ARL-RP-0329). 2011.

[22] Hisley DM, Gurganus JC, Drysdale AW. Experimental Methodology Using Digital Image Correlation to Assess Ballistic Helmet Blunt Trauma. J Appl Mech 2011;78:51022. doi:10.1115/1.4004332.

[23] McCrum NG, Read BE, Williams E. Anelastic and dielectric effects in polymeric solids. 2nd ed. New York: Dover Publications; 1991.

[24] Hu W, Hsieh AJ. Phase-mixing and molecular dynamics in poly(urethane urea) elastomers by solid-state NMR. Polymer 2013;54:6218–25. doi:10.1016/j.polymer.2013.09.010.

[25] Hu W, Patil N V., Hsieh AJ. Glass transition of soft segments in phase-mixed poly(urethane urea) elastomers by time-domain 1H and 13C solid-state NMR. Polymer 2016;100:149–57. doi:10.1016/j.polymer.2016.08.015.

[26] Duggal AR, Rogers JA, Nelson KA. Real-time optical characterization of surface acoustic modes of polyimide thin-film coatings. J Appl Phys 1992;72:2823–39. doi:10.1063/1.351535.

[27] O'Sickey MJ, Lawrey BD, Wilkes GL. Structure-property relationships of poly(urethane urea)s with ultra-low monol content poly(propylene glycol) soft segments: I. Influence of soft segment molecular weight and hard segment content. J Appl Polym Sci 2002;84:229–43. doi:10.1002/app.10168.

[28] Gama BA, Lopatnikov SL, Gillespie JW. Hopkinson bar experimental technique: A critical review. Appl Mech Rev 2004;57:223. doi:10.1115/1.1704626.

[29] Mayo MJ, Nix WD. A micro-indentation study of superplasticity in Pb, Sn, and Sn-38 wt% Pb. Acta Metall 1988;36:2183–92. doi:10.1016/0001-6160(88)90319-7.

[30] Tabor D. A Simple Theory of Static and Dynamic Hardness. Proc R Soc A Math Phys Eng Sci 1948;192:247–74. doi:10.1098/rspa.1948.0008.

[31] Hunter SC. The Hertz problem for a rigid spherical indenter and a viscoelastic half-space. J Mech Phys Solids 1960;8:219–34. doi:10.1016/0022-5096(60)90028-4.

[32] Kharaz AH, Gorham DA. A study of the restitution coefficient in elastic-plastic impact. Philos Mag Lett 2000;80:549–59. doi:10.1080/09500830050110486.

[33] Calvit HH. Experiments on rebound of steel balls from blocks of polymer. J Mech Phys Solids 1967;15:141–50. doi:10.1016/0022-5096(67)90028-2.

[34] Constantinides G, Tweedie C, Holbrook D, Barragan P, Smith J, Van Vliet K. Quantifying deformation and energy dissipation of polymeric surfaces under localized impact. Mater Sci Eng A 2008;489:403–12. doi:10.1016/j.msea.2007.12.044.

[35] Diani J, Gilormini P, Agbobada G. Experimental study and numerical simulation of the vertical bounce of a polymer ball over a wide temperature range. J Mater Sci 2014;49:2154–63. doi:10.1007/s10853-013-7908-2.

[36] Raphael T, Armeniades CD. Correlation of rebound tester and torsion pendulum data on polymer samples. Polym Eng Sci 1967;7:21–4. doi:10.1002/pen.760070105.

[37] Constantinides G, Tweedie CA, Holbrook DM, Barragan P, Smith JF, Van Vliet KJ. Quantifying deformation and energy dissipation of polymeric surfaces under localized impact. Mater Sci Eng A 2008;489:403–12.

[38] Hsieh AJ, Eliason JK, Nelson KA. Impulsive Stimulated Scattering Measurements of Select Model Transparent Elastomers. ARTL-TR-6167 2012.

[39] Schaefer J, Stejskal EO, Perchak D, Skolnick J, Yaris R. Molecular mechanism of the ring-flip process in polycarbonate. Macromolecules 1985;18:368–73. doi:10.1021/ma00145a012.

Molecular Influence in High-Strain-Rate Microparticle Impact Response of Poly(urethane urea) Elastomers

David Veysset, Alex J. Hsieh, Steven E. Kooi, and Keith A. Nelson

Supplementary Information

The maximum penetration depth in PUUs was measured and averaged over the range of the highest impact speeds studied (600 to 800 m/s), so as the coefficient of restitution data averaged over the same speed range. Both the trends in penetration depth and coefficient of restitution highlight a better corroboration with the effective hard segment content HS_{uu} (shown in Fig. 7) than HS_u (Fig. S1) among these select model PUUs impacted at high strain rates. This is consistent as the bidentate urea-urethane hydrogen bonding that contributes to greater phase mixing would presumably also undergo high-rate deformation-induced glass transition. As a result, HMDI moieties that are associated with the isolated hard segments dispersed among the soft domain matrix, yet not considered in the calculation of HS_u, would need to be taken into account with respect to their effective population. HS_{uu} aforementioned includes HMDI that reacts with PTMO to form the urethane linkages in addition to those reacted with the chain extender DETA to form the urea linkages [8].
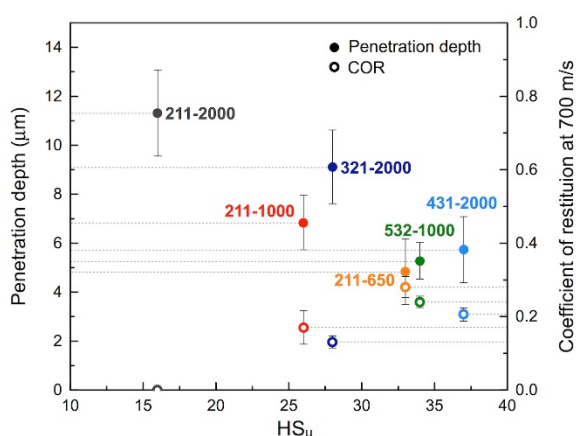

Fig. S1. Maximum penetration depth (solid-circles) and coefficient of restitution (open-circles) averaged for impact speeds between 600 m/s to 800 m/s as a function of HS_u.